Phase transition characteristics and piezoelectric properties of compositionally optimized alkaline niobate based ceramics

Jian Fu [a], Ruzhong Zuo [a,*], Xiaohui Wang [b], Longtu Li [b]

[a] *Institute of Electro Ceramics & Devices, School of Materials Science and Engineering, Hefei University of Technology, Hefei 230009, PR China*
[b] *State Key Lab of New Ceramics and Fine Processing, Department of Materials Science and Engineering, Tsinghua University, Beijing 100084, PR China*

A B S T R A C T

Lead-free $(Na_{0.52}K_{0.48-x})(Nb_{0.92-x}Sb_{0.08})O_3-x$LiTaO$_3$ ceramics with excellent dielectric and piezoelectric properties have been fabricated by ordinary sintering and their phase transition behavior, various electrical properties and temperature characteristics were investigated. The composition near $x = 0.0375$ exhibits a morphotropic phase boundary like behavior, and thus owns optimum electrical properties of $d_{33} = 395$ pC/N, $k_p = 52\%$, $\varepsilon_{33}^T = 2390$, $Q_m = 40$, $N_p = 3040$ Hz m and $T_c = 251\,^\circ$C. However, a strong temperature sensitivity in these compositions was observed as a result of the change of spontaneous polarization vectors or domain states, depending on the location of PPT. Compositions close to the tetragonal side exhibit much less temperature dependence, suggesting processing solutions to these obstacles.

© 2009 Elsevier B.V. All rights reserved.

1. Introduction

In recent years the Li, Ta and Sb modified $(Na,K)NbO_3$ (NKN) piezoelectric compositions [1–6] have gained much attention, being considered as one of the most potential lead-free candidates. Their excellent dielectric, piezoelectric and electromechanical properties have been comparable to those of some commercial $Pb(Zr,Ti)O_3$ (PZT) systems. Compared to tungsten bronze structured and bismuth layer structured lead-free compositions, and even $(Bi_{0.5}Na_{0.5})TiO_3$ based perovskite compositions, they also have obvious advantages. It is known that Li, Ta and Sb have been found to make different contributions to the electrical properties. For example, the $LiNbO_3$ or $LiTaO_3$ modified NKN ceramics tend to have enhanced piezoelectric properties by forming a morphotropic phase boundary (MPB) [7–9] (actually called as polymorphic phase boundary (PPB) in this system) near room temperature, and increased Curie temperatures (T_c), while the $LiSbO_3$ modified NKN ceramics tend to own reduced T_c although their piezoelectric properties can be improved more markedly [10,11]. In addition, it was reported that the dielectric properties have been merely limitedly promoted in the Li and/or Ta modified NKN ceramics while the $LiSbO_3$ or Sb modified NKN ceramics exhibit significantly enhanced dielectric constants. Therefore, it is believed that the compositional design or the addition of Li, Ta and Sb in an appropriate way is crucial in developing high-performance NKN based piezoelectric ceramics.

On the other hand, a few issues have been noticed almost while the advantages of NKN based compositions were recognized. In addition to the processing difficulties, and weak mechanical strength [12–14], the origin concerning their high piezoelectric activities has attracted much attention. Although pure NKN compositions have classical MPBs between two orthorhombic ferroelectric phases similar to those in widely used PZT systems, the addition of Li, Ta and Sb simply shifts a polymorphic phase transition (PPT, temperature at PPT called as T_{o-t}) existed in a pure NKN to lower temperatures, such that a two-phase coexistence zone or a PPB can be realized as the T_{o-t} is located at room temperature. This kind of PPB causes the NKN based compositions to have stronger temperature sensitivity [15–18] although it can promote piezoelectric activities like an MPB, owing to the increased amount of spontaneous polarization vectors.

Therefore, the purpose of this study is to manufacture NKN based lead-free piezoelectric ceramics with significantly enhanced dielectric and piezoelectric properties by compositional design. For this purpose, a suitable amount of Sb was added into NKN composition to increase the covalency of total compositions by taking into account the compromise between the properties and the Curie temperature. At the same time, $LiTaO_3$ was employed to form new solid solutions with a PPT near room temperature. In addition, the phase structure transition, electrical properties and temperature characteristics of solid solution ceramics were explored in combination with discussions on crystal or domain structures.

2. Experimental

A conventional solid-state method was used to fabricate lead-free piezoelectric ceramics with compositions of $(Na_{0.52}K_{0.48-x})(Nb_{0.92-x}Sb_{0.08})O_3-x$LiTaO$_3$

---

* Corresponding author. Tel.: +86 551 2905285; fax: +86 551 2905285.
E-mail address: piezolab@hfut.edu.cn (R. Zuo).

(NKNS8–xLT). High-purity oxides and carbonates, Nb_2O_5 (99.5%), Ta_2O_5 (99.9%), Sb_2O_3 (99.9%), Na_2CO_3 (99.8%), K_2CO_3 (99.0%) and Li_2CO_3 (99.9%), were used as the starting materials. After mixing, the powder mixtures were calcined twice at 850 °C for 5 h. The calcined powders were then milled again for 24 h together with 0.5 wt% PVB binder. After compaction, disk specimens were sintered in air at 1060–1120 °C for 3 h. For electrical measurements, silver paste was screen printed and then fired at 550 °C for 30 min. The electric poling was performed at 110 °C in a silicone oil bath by applying a dc field of ∼2 kV/mm for 15 min and the electric field was maintained during cooling.

The crystal structure was examined by an X-ray diffractometer (D/Mzx-rB, Rigaku, Japan) using a Cu Kα radiation. Dielectric properties were measured as a function of temperature by an LCR meter (Agilent E4980A, USA) equipped with an oven and a temperature box filled with liquid nitrogen. Polarization was measured under an alternating electric field using a ferroelectric measuring system (Precision WorkStation 2000, USA). The piezoelectric strain constant d_{33} was measured by a Belincourt-meter (YE2730A, Sinocera, Yangzhou, China). The planar electromechanical coupling factor k_p and the mechanical quality factor Q_m were determined by a resonance–antiresonance method with an impedance analyzer (PV70A, Beijing Band ERA Co., Ltd., China). The poled samples were annealed at different temperatures for 5 min and the d_{33} values were then measured again after being cooled to room temperature.

3. Results and discussion

The XRD patterns of NKNS8–xLT ceramics are shown in Fig. 1. No noticeable secondary phases can be detected as a few amount of Sb and $LiTaO_3$ diffuse into the perovskite lattice of NKN, although $(Na,K)SbO_3$ and $LiTaO_3$ have a lithium niobate structure while NKN has a perovskite structure. However, a change of the crystal structure at room temperature happens. The NKNS8-0.01LT ceramics exhibit a pure orthorhombic structure like undoped NKN. With an increase in the LT content, the crystal structure transforms from an orthorhombic symmetry to a tetragonal symmetry. It can be estimated that the structure transition zone is approximately at $0.0275 < x < 0.0375$. When $x > 0.0375$, the materials have a pure tetragonal structure. According to the definition of the MPB, a composition range can be identified at $0.0275 < x < 0.0375$ where two phases can coexist. Compared to NKN–xLT systems [19], the phase-coexisted compositions in this study contain less LT, because the addition of both Sb and LT shifts T_{o-t} to lower temperatures. On the tetragonal side, it can be seen that the tetragonality c/a increases with x as can be seen from the split $(0\,0\,2)$ and $(2\,0\,0)$ peaks. The tetragonal perovskite phases (ABO_3) usually have a tolerance factor (TF) more than 1 because too small B-site ions are easily off-center. The enhanced tetragonality is thus probably associated with the increase in TF. However, Ta^{5+} has similar ionic sizes as Nb^{5+} and Sb^{5+} (CN = 6, R_{Ta} = 0.64 Å, R_{Sb} = 0.61 Å, R_{Nb} = 0.64 Å), the ionic radius

Fig. 2. Dielectric constants at 10 kHz as a function of temperature for NKNS8–xLT ceramics as indicated and insets are the curves of both T_c and T_{o-t} changing with the LT content x, and the curves of dielectric constants at 10 kHz with temperature in the range of −55 to 180 °C, respectively.

of Li^+ is less than that of Na^+ and K^+ (CN = 12, R_{Li} = 1.25, R_{Na} = 1.39 Å, R_K = 1.64 Å) [20]. Therefore, the substitution of LT does not increase the TF of solid solutions but tends to decrease it if Goldschmit equation $(TF = (rA + rO)/\sqrt{2}(rB + rO))$ is used for its calculation [21]. It seems that why the addition of LT tends to increase the tetragonality cannot be well explained by the Goldschmit tolerance factor. This observation is unusual for a few perovskite systems such as $Pb(Mg_{1/3}Nb_{2/3})O_3$–$PbTiO_3$ (PMN–PT), $BiFeO_3$–PT, etc. The reason for this then could be that in NKNS–xLT systems two phases participating in forming solid solutions have two totally different crystal structures such that the perovskite lattice of NKNS8 compositions is more and more heavily distorted with the addition of LT. It may be carefully presumed that the Goldschmit tolerance factor does not fit these cases.

The temperature dependence of the dielectric constant of the NKNS8–xLT ceramics at 10 kHz is indicated in Fig. 2. Similar to pure NKN, the NKNS8–xLT compositions exhibit two phase transitions above room temperature, corresponding to an orthorhombic–tetragonal transition and a tetragonal–cubic transition when $x < 0.0275$. With increasing x, T_c increases slightly, probably associated with the increased tetragonality, while T_{o-t} decreases almost linearly such that only one phase transition above room temperature can be observed when $x > 0.0375$. It can be clearly seen from the inset of Fig. 2 (Up-left) that how T_{o-t} and T_c change with the content of LT. The tetragonal zone is thus broadened. Particularly, T_{o-t} is moved downwards below room temperature by changing the composition such that a MPB-like boundary can be formed (down-right in Fig. 2). Because the dielectric constants are measured during heating, T_{o-t} seems a little higher than that determined by XRD, for example, when $x = 0.0375$, the corresponding T_{o-t} is estimated at 40 °C, not exactly at room temperature (25 °C). Moreover, it can be found that PPB in all compositions is diffuse or in a wide temperature range. This could be the reason why two phases can exist simultaneously at ambient temperature in NKN based compositions as T_{o-t} is moved to near room temperature. Fig. 3 schematically depicts how the phase transition behavior responds to either temperature or composition. It can be easily observed that the PPT is diffuse within a broad temperature range, meaning that the transition from orthorhombic to tetragonal phases is continuous and gradual. This kind of diffuse PPT, which behaviors like a relaxor ferroelectric phase transition, is probably attributed to the locally fluctuated compositions or coexisted multi-phases with varying PPT temperatures. It is thus

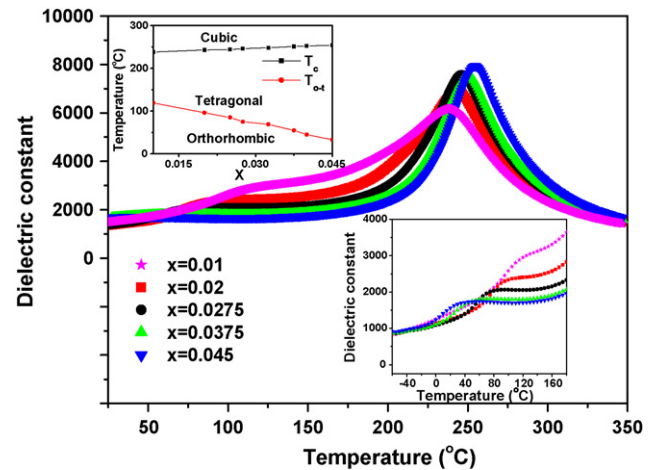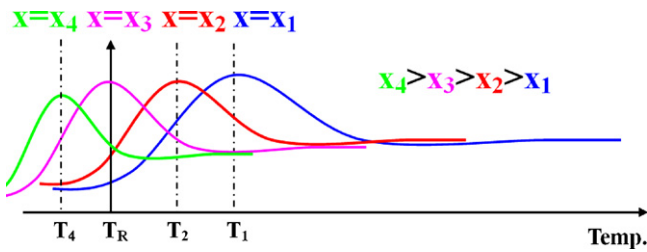**Fig. 1.** X-ray diffraction patterns of NKNS–xLT ceramics with different LT contents as indicated.

Fig. 3. Schematic diagram showing how the polymorphic phase structure transition changes with temperature and composition for NKNS8–xLT compositions; note that T_1, T_2, T_R and T_4 are the central temperatures of the PPT for compositions with $x = x_1$, x_2, x_3 and x_4, respectively.

understandable that the diffuseness of the PPT could result in two-phase coexistence at a certain temperature. For compositions with different x, the central temperatures of their PPTs are different. Supposed that the samples are composed of 50% orthorhombic and 50% tetragonal phases at the central temperature, for example, $x = x_3$, the compositions with $x < x_3$ (x_1 and x_2) at T_R should be composed of more orthorhombic phases and less tetragonal phases. On the contrary, the compositions with $x > x_3$ (x_4) should be composed of less orthorhombic phases and more tetragonal phases. Therefore, with continuously changing the composition (x), the materials will undergo a transition from a single orthorhombic phases to a mixture of orthorhombic and tetragonal phases and finally to a single tetragonal phase. Within the two-phase zone, the percentage of tetragonal phases increases with increasing x. The boundary between single orthorhombic phases and single tetragonal phases owing to the composition change is thus analogous to a traditional MPB in a sense of the two-phase coexistence. The two-phase coexistence could lead to the increased number of spontaneous polarization vectors in a certain composition.

In addition, the diffuse phase transition characteristics at T_c can also be observed in all NKNS8–xLT samples, as shown in Fig. 4. The diffuseness of the phase transition can be determined from the modified Curie–Weiss law $1/\varepsilon - 1/\varepsilon_m = C^{-1}(T - T_m)^\gamma$ where γ is the degree of diffuseness, C is the Curie–Weiss constant, and T_m is the phase transition temperature corresponding to the maximum dielectric constant ε_m. The parameter γ varies in the range from 1 for a normal ferroelectric to 2 for an ideal relaxor ferroelectric, which is equal to the slopes of linearly fitted lines in Fig. 4. Pure NKN samples were taken for comparison [22]. It can be found that
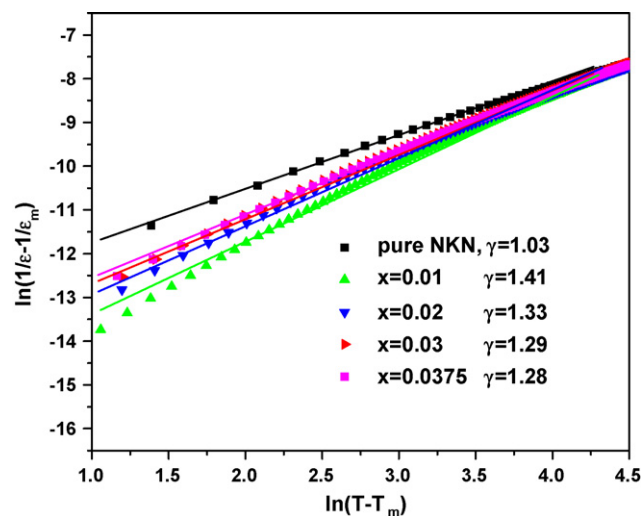

Fig. 4. Plot of $\ln(1/\varepsilon - 1/\varepsilon_m)$ vs. $\ln(T - T_m)$ for the NKNS8–xLT ceramics. The symbols denote experimental data, while the solid lines denote the least-squares fitting lines to the modified Curie–Weiss law.
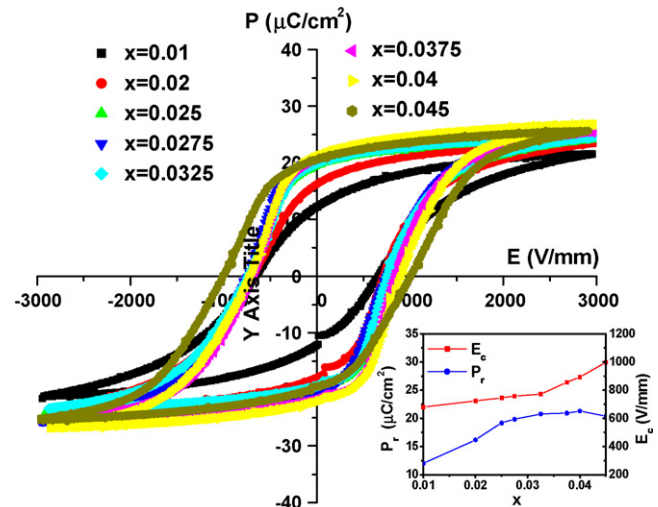

Fig. 5. Polarization vs. electric field hysteresis curves of NKNS8–xLT ceramics with different x; Insets are the curves of polarization (P) and coercive field (E_c) for different compositions.

its γ is 1.03, indicating that it is a normal ferroelectric. However, γ suddenly increases to 1.41 for NKNS8-0.01LT compositions and then starts to decrease with a further increase in x (1.28 for $x = 0.0375$). This means that the increase in γ is attributed to the addition of Sb^{5+}, that is to say, the addition of Sb^{5+} reduces the Curie temperature and induces a diffuse phase transition at the same time. This could be explained as that the occupation of Sb^{5+} at B sites increases the disordered degree of B-site ions. Noticeably, further addition of LT however decreases the diffuseness of the system although A-site or B-site ions may become more complex. This is probably owing to the increased tetragonality after the addition of LT. The enhanced c/a values implies that B-site ions could be more off-center along c axis, meaning an increase in ordered degrees to a certain extent. On the other hand, the increase in the Curie temperatures owing to the addition of LT also helps increase the ordered arrangement of A- and/or B-site ions at room temperature.

Fig. 5 indicates the variation of polarization with an alternating electric field for undoped NKNS8–xLT ceramics. Typical hysteresis loops were obtained for all samples with varying remnant polarization (P_r) and coercive field (E_c) as shown by the down-right inset. The compositions exhibit typically soft piezoelectric properties, i.e., a higher P_r ($\sim 20 \mu C/cm^2$) and a lower E_c (<1 kV/mm). It can be seen that P_r first increases slightly with increasing the LT content x, reaches a plateau approximately at $x = 0.0375$ and then slowly decreases with further increasing x. On the contrary, E_c exhibits only a slight rise before $x = 0.0375$ and then a fast increase after that. That is to say, both E_c and P_r exhibit a change near the two-phase coexistence zone as shown in Fig. 1. It should be understood that the compositions near a PPT own a larger P_r owing to an increase in the number of spontaneous polarization vectors. E_c is a variable accounting for how difficultly or easily the domains switches. This may depend on the type of domain structures to a certain degree. 90° domains predominantly existing in a tetragonal phase switches with an electric field more difficultly than 180° domains probably appearing in an orthorhombic phase. This point will be discussed infra. In the tetragonal zone, the tetragonality increases with increasing x as discussed in Fig. 1. The increase in E_c can be associated with the increased tetragonality probably inducing the formation of more 90° domains. This phenomenon has been observed in a few systems such as $PbZrO_3$–$PbTiO_3$ and PMN–PT, etc.

Fig. 6 shows the piezoelectric and electromechanical properties as well as the dielectric properties as a function of the LT content for poled NKNS8–xLT ceramics. Generally speaking, the dielectric con-
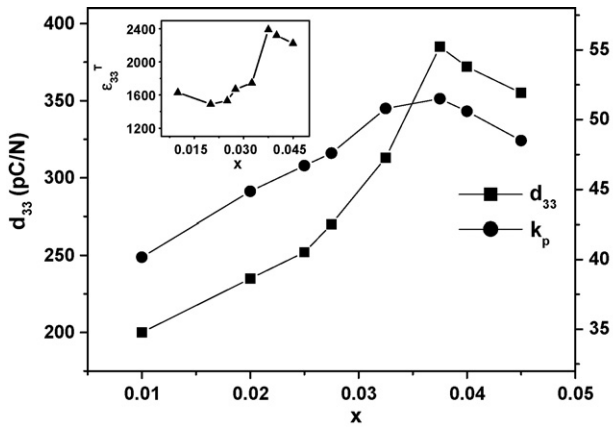
Fig. 6. Piezoelectric and electromechanical properties of poled NKNS8–xLT ceramics; Inset is the dielectric constants ε_{33}^{T} changing with x.

Fig. 7. Mechanical quality factor and frequency constant of poled NKNS8–xLT ceramics.

stant ε_{33}^{T} of NKNS8–xLT compositions is higher than that of pure NKN (ε_{33}^{T} ~500 for hot pressed NKN ceramics [23]) (see inset of Fig. 6). For example, the ε_{33}^{T} of NKNS8-0.01LT is as high as 1600. This partially results from the increased disorder in a perovskite structure induced by the substitution of Sb for Nb. Moreover, Sb has a higher electronegativity than Nb, making more contribution to the polarity of the composition. However, it can be seen that with further increasing the LT content x, the ε_{33}^{T} first slightly decreases, corresponding to the decrease in the disordered degree as discussed above, and then rapidly rise, reaching a maximum at $x = 0.0375$, owing to the typical effect of two-phase coexistence. Whether the origin of the two-phase coexistence in NKN based compositions and PZT based compositions is the same or not is still uncertain. However, one could imagine that the two-phase coexistence could be due to the diffuse PPT near room temperature, which is rather sensitive to temperature. Furthermore, the piezoelectric strain constant d_{33} and the planar electromechanical coupling coefficient k_p in Fig. 6 exhibit a typically compositional dependence as seen in most of the MPB compositions, reaching the maxima of ~395 pC/N and 52% at $x = 0.0375$, respectively. The excellent piezoelectric and electromechanical properties can be attributed to two aspects: on the one hand, the higher electronegativities of Sb and Ta compared to Nb make the structure more covalent, which effectively improves the dielectric and piezoelectric activities; on the other hand, the addition of LiTaO$_3$ can generate new solid solutions some of which may exhibit two-phase coexistence as T_{o-t} lies near room temperature, playing a key role in the enhancement of piezoelectric performances.

The mechanical quality factor Q_m and the frequency constant N_p as a function of x are shown in Fig. 7. It can be seen that both Q_m and N_p display opposite responses to the compositional change. They are generally higher at the orthorhombic side than at the tetragonal side, reaching the minima of $Q_m = 40$ and $N_p = 3040$ Hz m at $x = 0.0375$, respectively. It is known that Q_m characterizes the internal friction in a grain and is mainly related to the domain motion. The compositions with $x = 0.0375$ may exhibit a coexistence state of orthorhombic and tetragonal ferroelectric domains, where the increased kinds or numbers of domains in these compositions may ease the domain motion driven by an external electric field. This behavior is similar to that the increased number of spontaneous polarization vectors in MPB compositions makes the orientation of polarization vectors easier during electric poling. Therefore, the MPB compositions usually have higher dielectric and piezoelectric activities ("soft" characteristics). Similarly, N_p shows the same tendency as Q_m, which is proportional to the elastic hardness. Additionally, it can be found that the N_p in all NKNS8–xLT
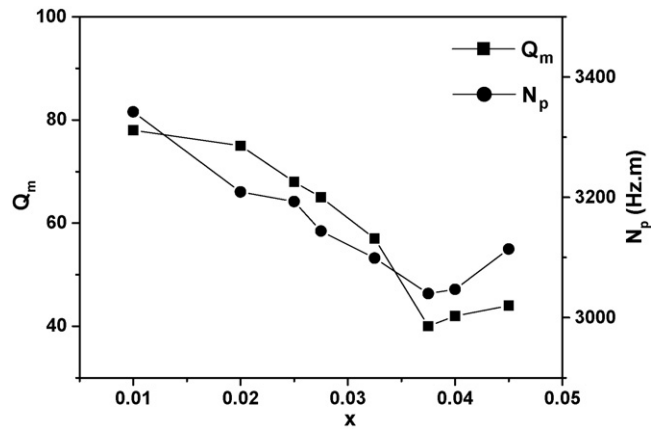
compositions is over 3000 Hz m, higher than that of PZT ceramics (2000–2400 Hz m), probably because of the lower density of these compositions (theoretical density for pure NKN is 4.51 g/cm^3) compared to that of PZT systems. Such a high frequency constant is advantageous to high frequency applications.

The d_{33} values were measured at room temperature after annealing the samples at varying chosen annealing temperatures for 5 min. These values were normalized through dividing them by initial values of respective samples. Normalized d_{33} values as a function of temperature for different compositions are shown in Fig. 8. It can be seen that the d_{33} values exhibit a fast drop after the samples undergo a PPB from an orthorhombic phase to a tetragonal phase. Before complete depolarization comes due to a ferroelectric–paraelectric phase transition at the Curie temperatures, the piezoelectric properties for samples with different x exhibit a drop of different degrees, for example, 20% for NKNS8-0.02LT, 15% for NKNS-0.0375LT but only 6% for NKNS-0.045LT. It seems that the loss of piezoelectric properties after annealing decreases at the same temperature with increasing x. It can be understood in the way that these differences result from the different ratios of orthorhombic to tetragonal phases in the compositions near a PPT. From the crystallographic point of view, there are 12 domain orientation states in an orthorhombic perovskite structure because its spontaneous polarization is along $\langle 1\,1\,0 \rangle$ direction
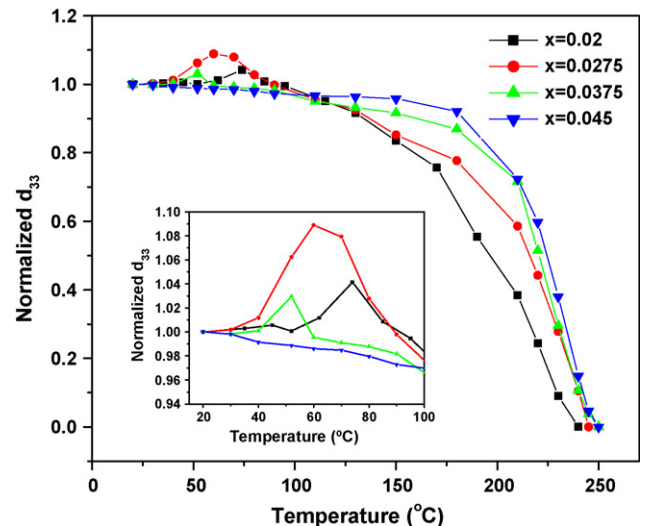

Fig. 8. Temperature dependence of piezoelectric properties of poled NKNS8–xLT ceramics. Inset is the locally enlarged plot in the temperature range of 20–100 °C.

such that 180° and non-180° domains may predominantly exist in the grain. However, there are 6 domain orientation states in a tetragonal perovskite structure because its spontaneous polarization is along $\langle 1\,0\,0 \rangle$ direction so that 90° and 180° domains may be mainly formed. The 18 spontaneous polarization directions in a PPT composition may ease the domain switching during poling. However, a high degree of alignment of ferroelectric dipoles for PPT compositions after poling owing to the two-phase coexistence can be degenerated when those compositions undergo a phase transition during annealing. On the one hand, because 180° domain switching does not cause any strains, it should be also more easily switched back during heating. On the other hand, the higher the $T_{o\text{-}t}$ is, the more the content of orthorhombic phases at room temperature in a PPT composition and the more the piezoelectric properties are degenerated because of the disappearance of the oriented orthorhombic domains at a high annealing temperature. It can be also expected that with increasing thermal cyclic times the piezoelectric properties tend to further decrease till they get stable as only stably oriented tetragonal domains remain. By comparison, this issue can be avoided or alleviated in the compositions located on the tetragonal side. Therefore, from the viewpoint of practical applications, it is feasible to improve the temperature stability of piezoelectric properties by shifting the $T_{o\text{-}t}$ below room temperature or choosing a composition on the tetragonal side. Moreover, a small peak appears in the curves of temperature dependence of d_{33} for different compositions at the corresponding phase transition temperature, similar to the dielectric anomaly in the dielectric permittivity vs. temperature curves. The reason is that the d_{33} values are proportional to the dielectric constant as described by $d_{33} = 2Q_{11}\varepsilon P_s$ [24], where Q_{11} is the electrostrictive coefficient, ε is the dielectric constant and P_s is the spontaneous polarization. These results may suggest a processing solution to these issues that $T_{o\text{-}t}$ should be moved downwards below room temperatures by some dopants or by choosing a tetragonal-side composition.

4. Summary

The conventionally sintered lead-free $(Na_{0.52}K_{0.48-x})(Nb_{0.92-x}Sb_{0.08})O_3$–$x$LiTaO$_3$ (NKNS8–xLT) piezo-electric ceramics exhibit excellent dielectric and piezoelectric properties of $d_{33} = 395$ pC/N, $k_p = 52\%$, $\varepsilon_{33}^T = 2390$, $Q_m = 40$, $N_p = 3040$ Hz m and $T_c = 251\,^\circ$C. The co-substitution of Sb and LT combines the contributions of Sb to the large dielectric constants owing to its high electronegativity, and of MPB-like crystal structures to high piezoelectric activities achieved by shifting a PPT to near room temperature. A remarkable compositional dependence of various electrical properties was observed, together with a detailed discussion on the temperature stability issues associated with the existence of the PPT, and on processing solutions from a crystallographic point of view.

References

[1] Y. Saito, H. Takao, T. Tani, T. Nonoyama, K. Takatori, T. Homma, T. Nagaya, M. Nakamura, Nature 432 (2004) 84.
[2] B.Q. Ming, J.F. Wang, P. Qi, G.Z. Zang, Appl. Phys. Lett. 101 (2007) 054103.
[3] D.M. Lin, K.W. Kwok, H.L.W. Chan, J. Phys. D: Appl. Phys. 40 (2007) 6060.
[4] Z.P. Yang, Y.F. Chang, L.L. Wei, Appl. Phys. Lett. 90 (2007) 042911.
[5] E.K. Akdogan, K. Kerman, M. Abazari, A. Safari, Appl. Phys. Lett. 92 (2008) 112908.
[6] J.G. Wu, T. Peng, Y.Y. Wang, D.Q. Xiao, J.M. Zhu, Y. Jin, J.G. Zhu, P. Yu, L. Wu, Y.H. Jiang, J. Am. Ceram. Soc. 91 (2008) 319.
[7] Y.P. Guo, K. Kakimoto, H. Ohsato, Appl. Phys. Lett. 85 (2004) 4121.
[8] E. Hollenstein, M. Davis, D. Damjanovic, N. Setter, Appl. Phys. Lett. 87 (2005) 182905.
[9] H.C. Song, K.H. Cho, H.Y. Park, C.W. Ahn, S. Nahm, K. Uchino, S.H. Park, H.G. Lee, J. Am. Ceram. Soc. 90 (2007) 1812.
[10] S.J. Zhang, R. Xia, T.R. Shrout, G.Z. Zang, J.F. Wang, J. Appl. Phys. 100 (2006) 104108.
[11] D.M. Lin, K.W. Kwok, K.H. Lam, H.L.W. Chan, J. Appl. Phys. 101 (2007) 074111.
[12] L. Egerton, D.M. Dillon, J. Am. Ceram. Soc. 42 (1959) 438.
[13] Z.S. Ahn, W.A. Schulze, J. Am. Ceram. Soc. 70 (1987) 18.
[14] Y.L. Wang, D. Damjanovic, N. Klein, E. Hollenstein, N. Setter, J. Am. Ceram. Soc. 90 (2007) 3485.
[15] S.J. Zhang, R. Xia, T.R. Shrout, Appl. Phys. Lett. 91 (2007) 132913.
[16] E. Hollenstein, D. Damjanovic, N. Setter, J. Eur. Ceram. Soc. 27 (2007) 4093.
[17] C. Lei, Z.G. Ye, Appl. Phys. Lett. 93 (2008) 042901.
[18] J.G. Wu, D.Q. Xiao, Y.Y. Wang, W.J. Wu, B. Zhang, J.G. Zhu, J. Appl. Phys. 104 (2008) 024102.
[19] Y.P. Guo, K. Kakimoto, H. Ohsato, Mater. Lett. 59 (2005) 241.
[20] R.D. Shannon, Acta Cryst. A32 (1976) 751.
[21] M. Johnsson, P. Lemmens, Crystallography and chemistry of perovskites, in: H. Kronmueller, S. Parkin (Eds.), Handbook of Magnetism and Advanced Magnetic Materials, John Wiley & Sons Ltd., New York, 2006, pp. 2098–2106.
[22] R.Z. Zuo, J. Rodel, R.Z. Chen, L.T. Li, J. Am. Ceram. Soc. 89 (2006) 2010.
[23] S.J. Zhang, R. Xia, T.R. Shrout, G.Z. Zang, J.F. Wang, Solid State Commun. 141 (2007) 675.
[24] B.M. Jin, J. Kim, S.C. Kim, Appl. Phys. A 65 (1997) 53.